

Additive Manufacturing of Directionally Heat Conductive Objects

Kulkarni P.M*, Karunakaran K.P*, Asim Tewari*, Fisseha Legesse*, Dhirendra Rana*, Alain Bernard**

*Rapid Manufacturing Laboratory, Department of Mechanical Engineering,
Indian Institute of Technology Bombay, Powai, Mumbai-400076, INDIA

**Virtual engineering for industrial engineering, IRCCyN, Ecole Centrale de
Nantes, France

REVIEWED

Abstract

Purpose: Directionally Heat Conductive (DHC) objects are also known as thermal cables. DHC objects used in cooling solid state devices as large heat sinks. This paper presents Additive manufacturing (AM) as a new method for realization of DHC objects. AM can produce DHC objects accurately, rapidly and economically.

Design/Methodology/Approach: It is very hard to realize DHC objects through conventional manufacturing. The authors describe the realization of metallic DHC objects using their AM process called Hybrid Layered Manufacturing (HLM). HLM, which uses GMAW deposition, can, in principle, produce DHC out of any metal for which welding wire is available. . Differential conductivity in HLM is achieved by appropriately distributing the air gaps among the beads. The air gap distribution depends on the layer thickness and step over increment.

Findings: The authors have demonstrated the ability of HLM to produce DHC objects for Al alloy 4043. The thermal conductivity achieved on two orthogonal directions was 100.496 and 129.740 W m⁻¹ K⁻¹ as against 163 W m⁻¹ K⁻¹ for solid metal. These are significant variations.

Research Limitations/Implications: HLM realize near net shape of DHC objects, further post processing namely machining is required.

Originality Value: AM Specifically HLM for realization of DHC objects

Keywords: Directional heat conductive (DHC), Additive Manufacturing (AM), Hybrid Layered Manufacturing (HLM).

1. Introduction

Thermal conductivity of a material has great influence on its performance in heat transfer analysis, a material is normally assumed to be isotropic. Therefore, it is a common practice to evaluate the thermal conductivity at the average temperature and treat it as a constant in calculations [1]. This assumption is realistic for most materials, but some materials, such as laminated composites, are anisotropic. This anisotropy can be engineered to have directional conductivity. Such objects are known as *Directionally Heat Conductive (DHC)* objects. There are several applications of DHC in different fields.

The characteristics of a DHC object depend on the material composition and porosity or void along different directions. DHC objects find major applications as heat sinks in electronic packaging, especially for high voltage chips, packaging base plates, carrier plates of electronic box closures [2, 3]. In these applications, heat dissipation is important because modern integrated circuits and other powerful electronic parts generate a lot of heat.

H. Amiri et al. have reported the numerical solution for the steady state combined conductive-radiative heat transfer in an anisotropic participating medium within the irregular geometries [4]. Some of the engineering applications of such combined properties were mentioned in areas such as thermal transport in nano-materials, heat transfer through the semi-transparent, porous materials, multi-layered insulations, glass fabrication etc. [5]. Similarly DHC objects can be used as effective heat conductors in large, high speed electrical machines as housing jackets to extract the heat generated inside the stator. It can be also used for insulation in industrial furnaces to retain the heat [6]. Aerospace engines uses honeycomb structures which provides directional thermal conductivity as well as weight reduction.

Temperature rise in high speed electrical machine causes mechanical failures and irreversible demagnetization of permanent magnets. Initially temperature in high speed electrical machines was maintained by using forced air-cooling with external cooling fins often by a ventilator mounted on the shaft. At higher speeds, this may be very noisy and take up a fair deal of torque, so an independent cooling is required. This independent cooling is done by DHC housings.

Figure 1 shows the current methods of manufacturing DHC objects like bonding, sheet metal forming (folding and co-corrugation process), open and closed die forging, liquid forging, skiving, Powder Metallurgy (PM), Metal Matrix Composite (MMC) manufacture [7]. DHC objects manufactured by various process is shown in figure 1.

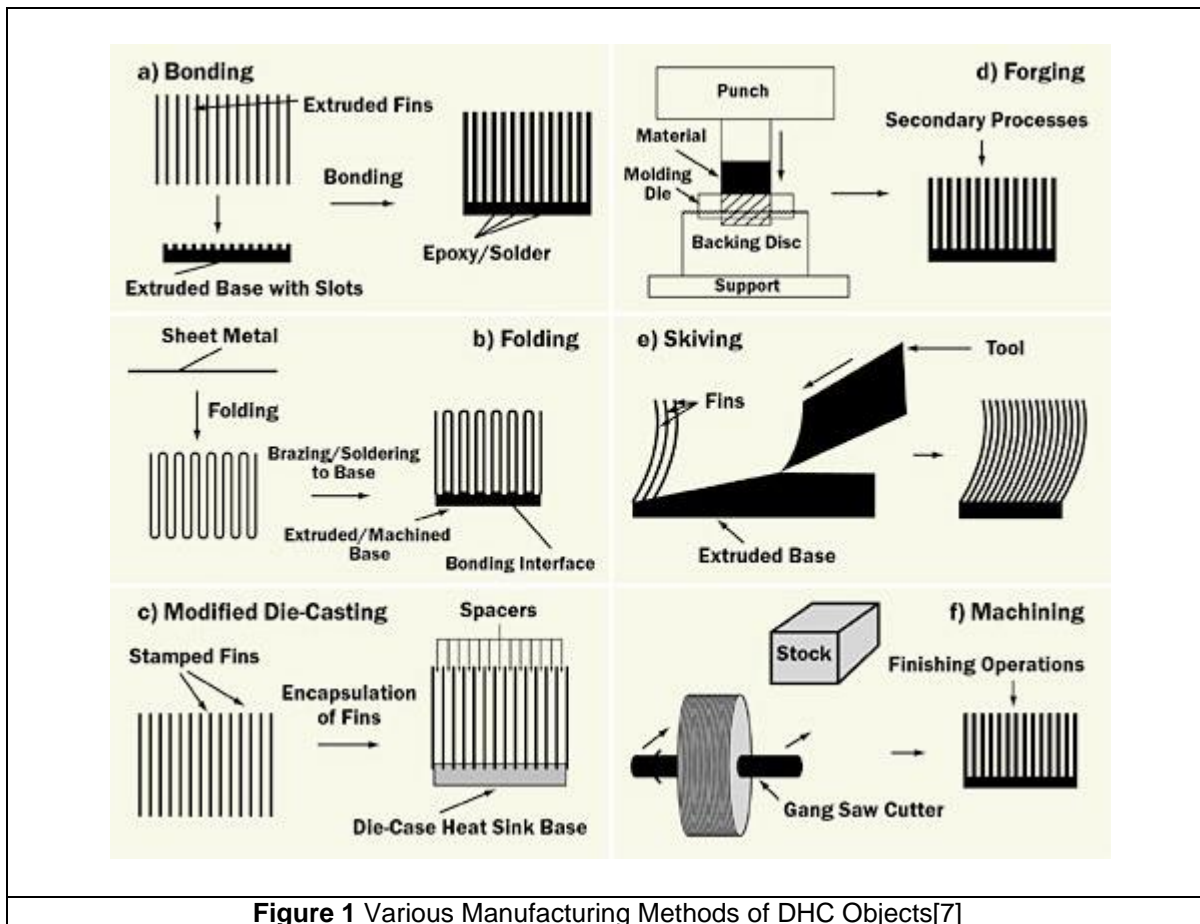
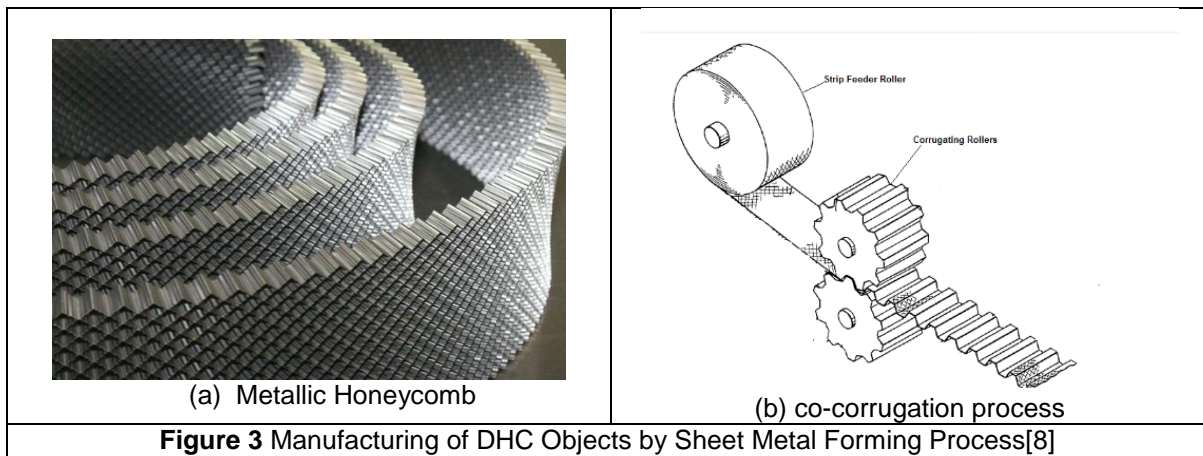
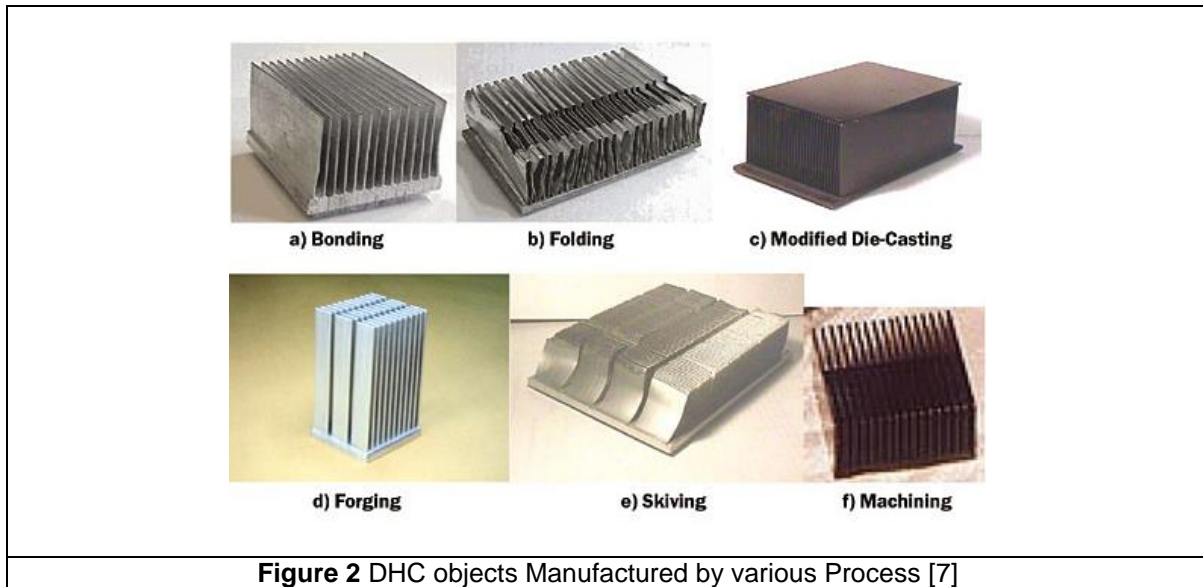


Figure 1 Various Manufacturing Methods of DHC Objects[7]

Honeycomb structure is manufactured by sheet metal forming method named as co-corrugation process. The unidirectional thermally conductive fibers are oriented in a direction parallel to the width of the formed sheet. There are various configurations of honeycomb structures, out of which hexagonal cells gives better directional thermal conductivity. Titanium honeycomb structure used for exhaust nozzles in aircraft is shown in figure 3(a) and this type of structure is manufactured by corrugation process shown in figure 3(b). This honeycomb structure finds major applications in military and commercial aircraft, automotive bodies, engine components, recreational equipment, and marine craft [8, 9].



MMC used to manufacture DHC vibration isolator imparting shock and vibration isolation. MMC can be manufactured by powder metallurgy and foil diffusion, both of them are solid based methods. Electroforming, stir casting, squeeze casting, spray deposition and reactive processing are the liquid based MMC manufacturing processes [10].

Heat sinks are manufactured by forging instead of casting, machining and extrusion. Forging is the most effective method to form complex shapes and also offers unique thermal advantages.

The part is formed under high pressure which controls the grain structure and results in improved thermal performance. The cold forging process results in a heat sink that yields a 14% improvement over the extruded and a 62% improvement over the die cast heat sink [11].

The above methods to produce DHC objects are hard and expensive as they are dominated by subtractive manufacturing [12]. With the advent of Additive Manufacturing (AM), manufacturing of DHC objects has become elegant and affordable. AM is inherently anisotropic. When this inherent anisotropy is engineered to meet the functional needs of a component, it is known as Functionally Gradient Materials (FGM). DHC is a special case of FGM.

Additive Manufacturing (AM) is the term given to a group of technologies that are capable of creating physical objects from computer aided design (CAD) files by incrementally adding material such that the objects “grow” from nothing to completion. Most of today’s AM technologies start with a CAD solid model which is sliced into thin layers. Each layer comprises a 2D cross section profile of the part which is then made layer by layer.

AM involves a number of steps that move from the virtual CAD description to the physical resultant part. Different products will involve AM in different ways and to different degrees. Small, relatively simple products may only make use of AM for visualization models, while larger, more complex products with greater engineering content may involve AM during numerous stages and iterations throughout the development process. Furthermore, early stages of the product development process may only require rough parts, with AM being used because of the speed at which they can be fabricated. At later stages of the process, parts may require careful cleaning and post-processing (including sanding, surface preparation and painting) before they are used, with AM being useful here because of the complexity of form that can be created without having to consider tooling [7].

The automated approach to creating objects from CAD files in the additive manner that AM allows is beginning to have a profound effect on how objects are made. Almost all manufactured objects that we see today are made with some form of tooling at some point – parts may be machined using a cutting tool or parts may be formed from a molding tool. The use of tooling imposes numerous restrictions such as design limitations, restrictive costs to prepare for manufacture and the need to create products at a single location prior to being shipped globally. AM technologies invariably require no tooling to create parts and this profoundly affects how products can be designed, tailored, made, distributed etc. [12].

Organization of Paper

In this paper authors give the introduction of HLM process, involvement of HLM technology in realization of DHC objects, characterization of DHC objects by using the heat conductivity testing. Finally authors give the conclusion in which they show unidirectional behavior of DHC objects.

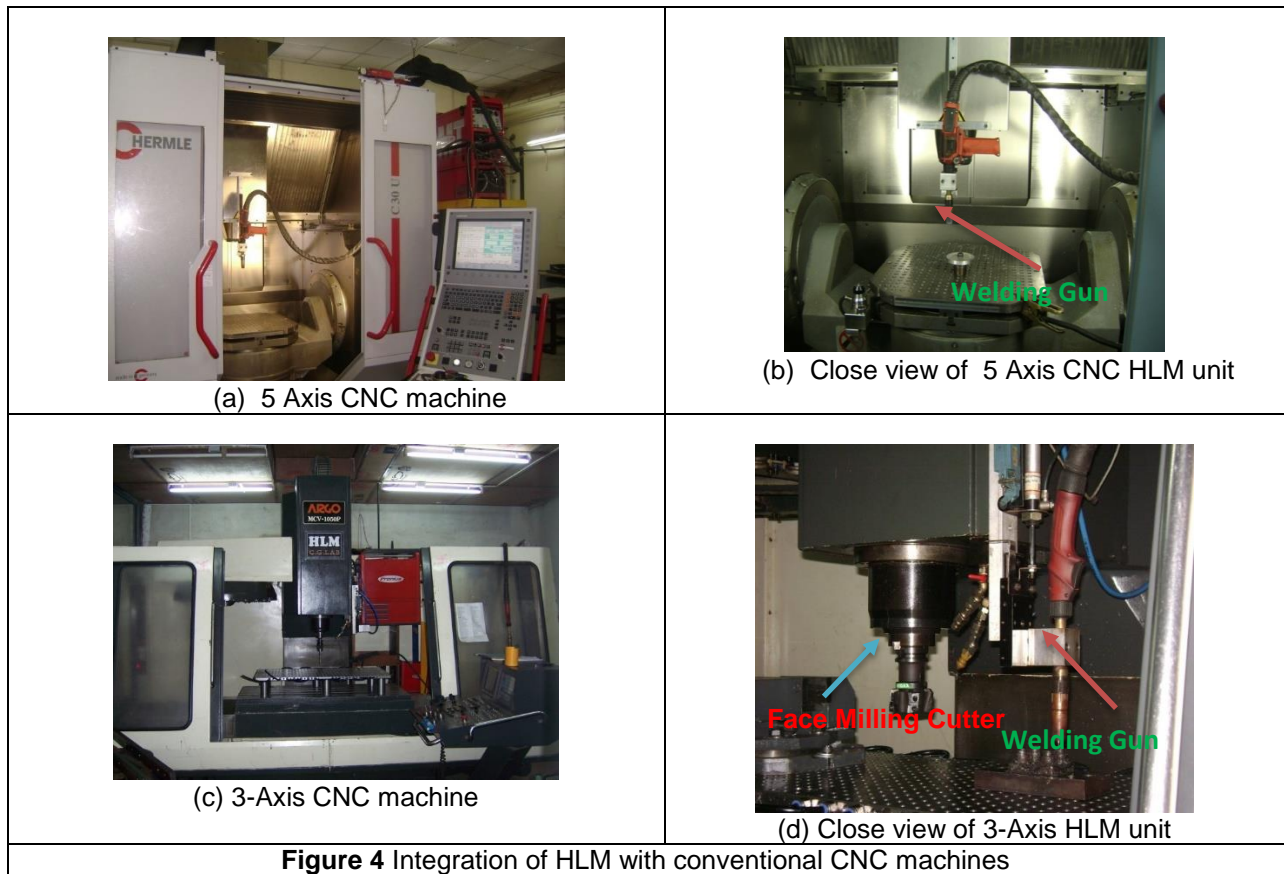
2. Hybrid Layer Manufacturing Process

Hybrid Layered Manufacturing (HLM) is a Rapid Manufacturing process which includes layer by layer deposition using *Gas Metal Arc Welding (GMAW)*. This deposition makes near-net shape of the object to be built which is then finish machined subsequently. Face-milling is done

after depositing each layer to remove oxidized surface and scallops. It also ensures z-accuracy of each layer. Integration of HLM with 5 axis and 3 axis CNC machines is shown in figure 4.

Arc weld deposition is faster and more economical by an order of magnitude than laser and electron beam processes (50-130g/min as against 2-10g/min). The surface quality is in the decreasing order for laser, electron beam and arc. Even the best surface obtained through AM is not adequate enough for direct use for very serious applications except in some medical applications where rough surface is favourable for tissue growth. If finish machining is necessary, then these marginal quality differences do not matter.

Subtractive processes can produce good quality parts but are slow; although the material removal by itself is fast, human efforts required for cutter path generation is the bottleneck. On the other hand, additive processes are fast but produce poor quality parts. The additive process focuses on speed while ensuring the desired material integrity. The resulting object is only near-net as no attention to the geometric quality is paid at the time of building it in layers. In HLM, the near-net shape is obtained with total automation. However, the subsequent two stages of stress relieving/ heat treatment and finish machining have fair amount of human intervention. In other words, HLM does not strive to achieve total automation but aims at optimal/ economical level of automation.



2.1 Methodology of HLM

The stages involved in building the metallic object using HLM is shown in figure 5.

- a. Geometric processing
- b. Building the near-net shape
- c. Stress relieving
- d. Finish machining

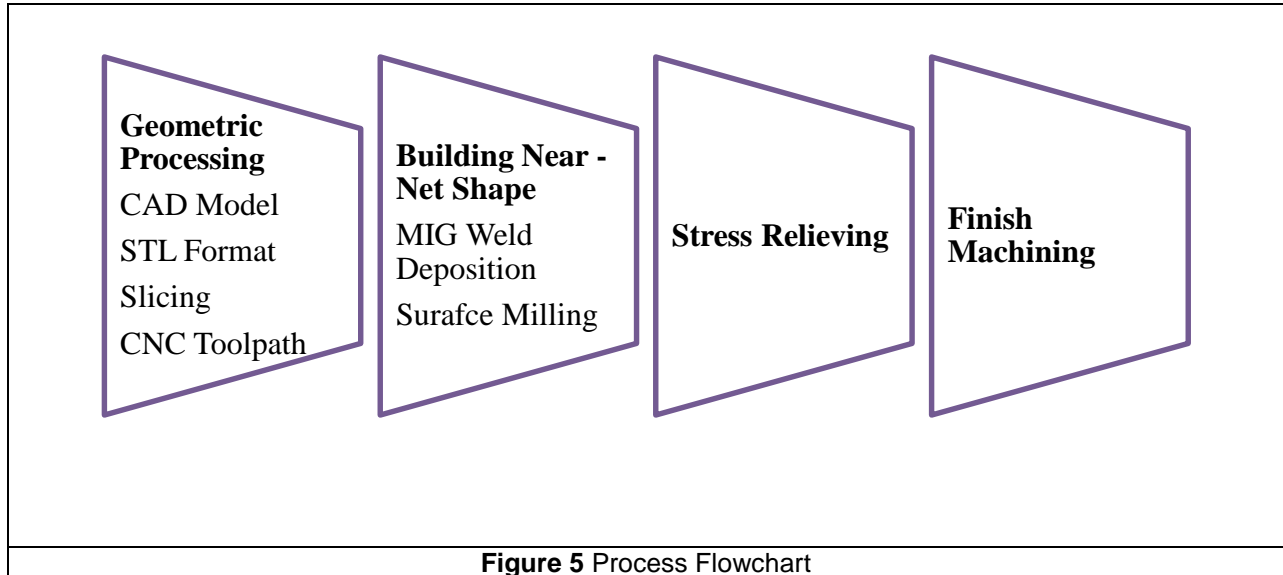


Figure 5 Process Flowchart

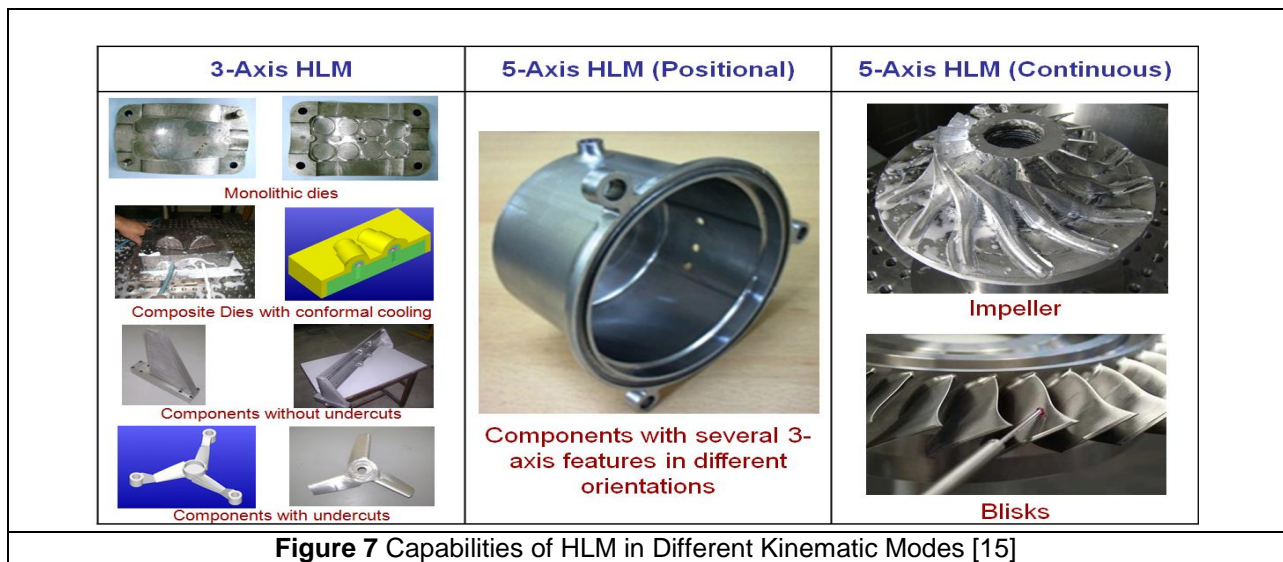
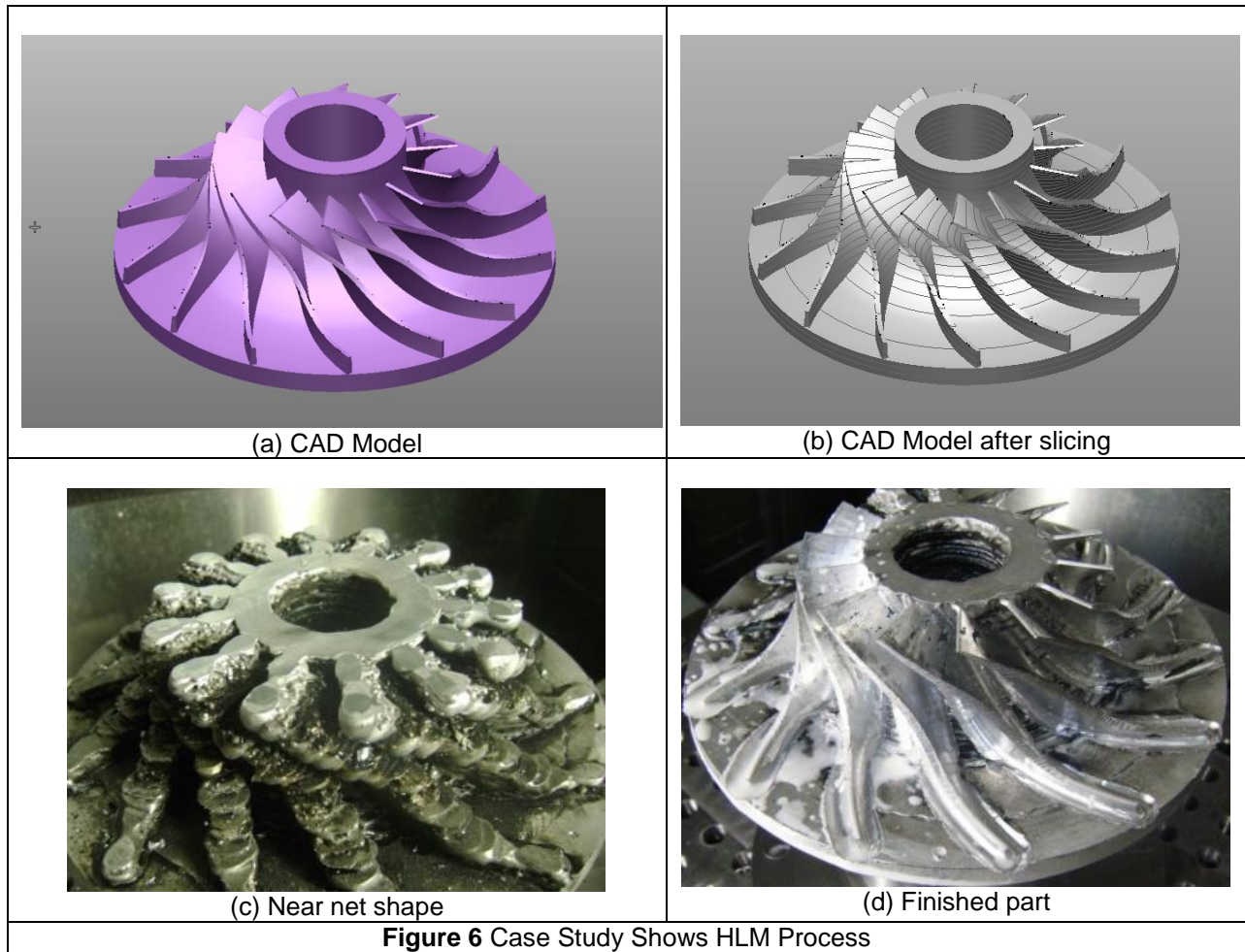
A case study of impeller which was manufactured using HLM process is shown below in figure 6.

2.2 Application

The various geometric capabilities of HLM, in its three kinematic modes of 3-axis, positional 5-axis and continuous 5-axis, are shown in figure 7. In 3 axis kinematics mode, we can manufacture parts by means of various approaches such as planar deposition, planar deposition with small undercuts, planar deposition after building the undercut, non-planar (conformal) deposition. HLM can be used to manufacture *Functionally Gradient Materials (FGM)* by using multiple welding torches at with different filler materials.

2.3 Advantages of HLM

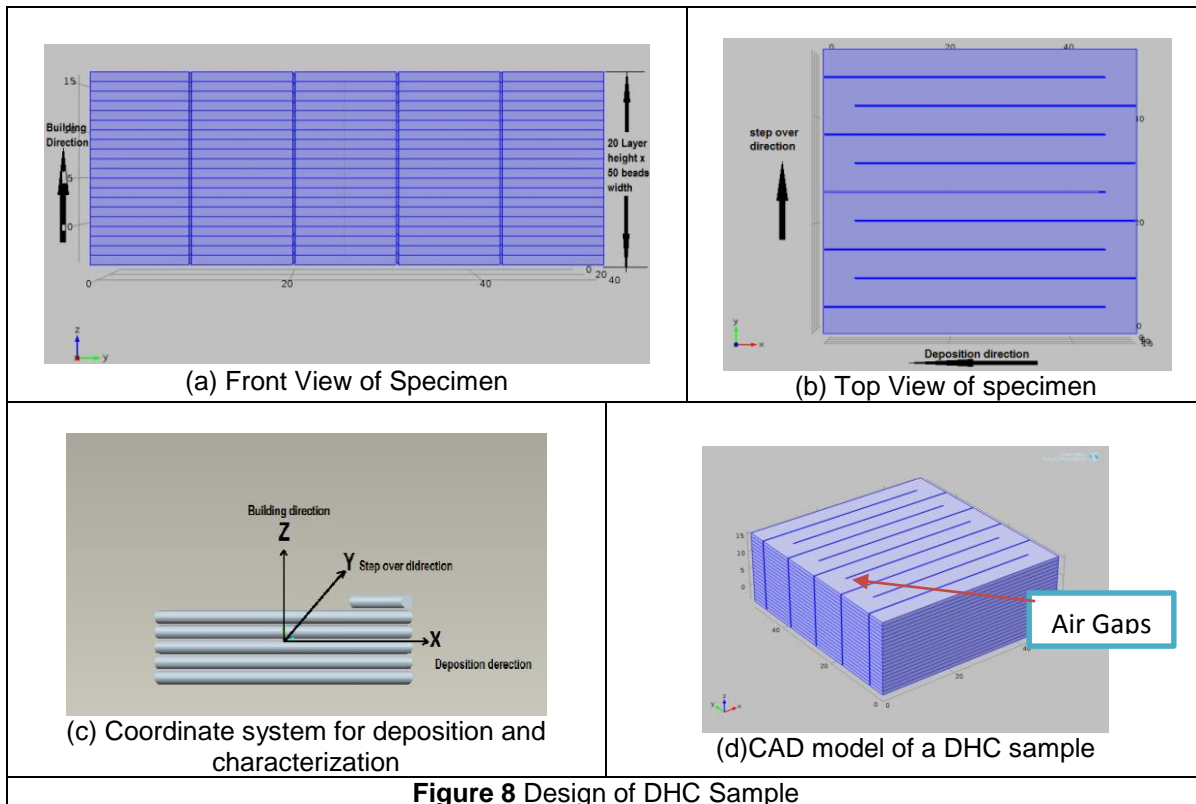
- i. Seamless integration of material addition and subtraction on the same platform
- ii. Totally automatic manufacture of the near-net shape
- iii. Use of economical, faster and safer GMAW as against laser and electron beam
- iv. Retrofittable to any existing CNC machine, independent of make and age
- v. Easy toggling between HLM mode and regular CNC machining mode



3. Realization of DHC Using HLM

A Cold Metal Transfer (CMT) 2700 welding machine and a 3-axis CNC machine were used for deposition and subtraction respectively. Three axis Cartesian coordinate system was adopted to identify the direction of deposition and directionally heat conductivity analysis. The X-axis (torch direction) is taken in the long travel of the weld torch, Z-axis is taken perpendicular to the surface of the substrate (weld direction) and Y-axis is taken in the stepover increments direction. Figure 8 illustrates the coordinate system used in deposition and characterization. The heat conduction was measured in the directions parallel and perpendicular to the air gaps in X and Y directions respectively.

The part was built by adopting zig-zag deposition. The deposition in the longitudinal direction was built on X-axis and the pitch was provided in a perpendicular direction. The pitch size was given by considering the air gaps between consecutive beads. Complete fusion between weld beads was prevented by providing a step over which is equal to half of the bead width plus the required air gap. The CAD model of the sample, with air gaps between each strip of layers, is shown below in figure 8 (d).



As shown in Table 1, during deposition different process parameters were taken into account. Wire speed which affects the bead width and thickness, and which in turn is affected by the rate of heat input, was controlled to minimize distortion of beads due to overheating during layer deposition. The torch speed which is another important welding parameter was controlled numerically to get a high precision in the weld bead size and to minimize heat distribution over a wider area [13]. If the torch speed is high, the bead width is thin and vice-versa. Therefore the

lowest wire speed and the highest torch speed within their stable operating ranges are chosen to preserve the required air gap. The other and the most important parameter which was critical to our specific experiment is the stepover increment. The size of the stepover determines the size of the air gaps. If the stepover is less than half of the width of the weld bead, complete fusion between adjacent weld beads will occur. The size of stepover was determined based on the required size of air gaps.

Variation of current with layer thickness is shown in figure 9. It shows that as current increases layer thickness also increases.

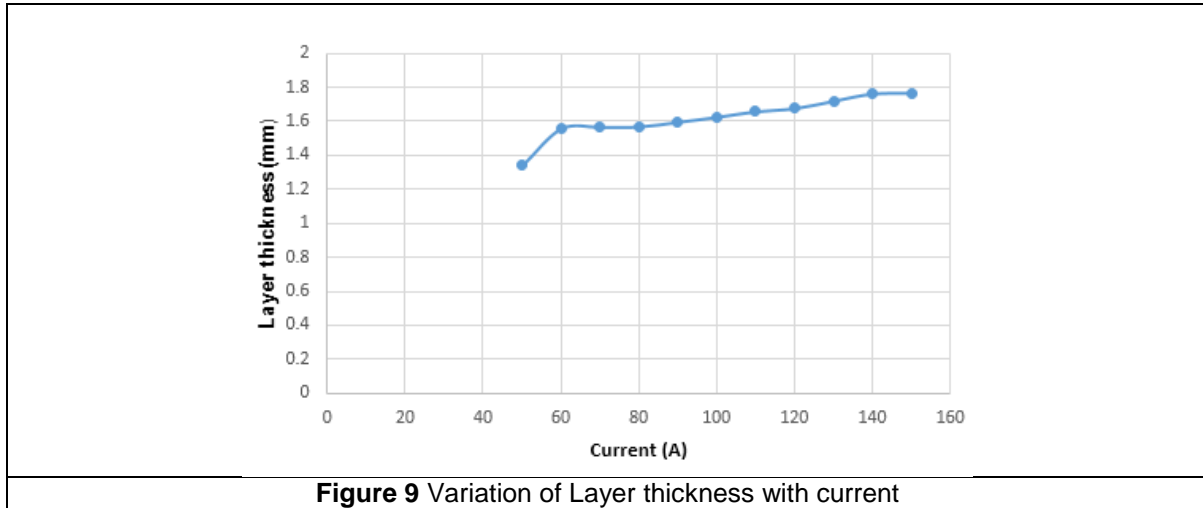


Figure 9 Variation of Layer thickness with current

The process parameters used during weld deposition are shown in table 1. The parameters are given based on the requirements of the final object.

Table 1 Welding Parameters for Al-Si

Layer thickness (mm)	1
Torch speed(mm/min)	850
Wire feed rate(m/min)	3.4
Welding wire diameter (mm)	1.2
Gas flow rate(l/min)	10-12
Shielding gas	Ar
Pitch	Bead width+ 0.25mm
Air gaps	0.25mm

4. Characterization of DHC

Characterization of DHC includes the thermocouple calibration which is used to plot a graph between temperature and voltage using which an equation is established. Furthermore a heat conduction test is performed to show the unidirectional heat flow.

4.1 Thermocouple Calibration

The necessity of the calibration is to establish an equation of curve that fits to the temperature versus voltage graph. This equation is applied to find out the unidirectional temperature drop or

rise in the sample along the specified directions. Hence a calibration setup was established to calibrate a thermocouple based on a manual by ASTM [14] using fixed reference temperature technique. If properly used, it is a convenient and inexpensive way to achieve the ice point, it can be reproduced with ease and with an exceptional accuracy of 0.0001°C [14]. Ice bath reference junction setup was established for this purpose as shown in figure 10. The ice bath is made up of a mixture of melting shaved ice and water. This is one of the most common reference junction techniques used in calibration. To avoid the errors due to melting of the ice at the bottom of the bath, consumed excess water was removed periodically and more ice was added, so that the ice level is maintained safely below the reference junctions.

The water level in the bath was checked and the apparatus was connected to a power supply. The temperature in the bath was initially set to 30°C to start heating. In normal mode, the temperature shown on the digital display is the actual temperature of the bath (T_B) against which the thermocouple sensor is to be calibrated. The ends of the thermocouple are connected to the digital multimeter and which was set to read voltage in mV. The other end of the thermocouple was dipped in ice bath. A stable temperature source was kept to maintain a constant temperature. The multimeter reading in millivolts was noted down for each 5°C increment in temperature from 30°C to 80°C. The most commonly used reference temperature is 0°C [13].

The multimeter reading in millivolt corresponding to the difference in temperature between the surroundings (ice) and the bath was recorded. The measured bath temperatures values (T_B) were plotted on Y-axis against the corresponding reading of emf (mV) values on X-axis, as shown in Fig.13. The slope and intercept of the curve-fitted were obtained from the equation correlated to the graph. The linear correlation coefficient (R), which measures the strength and the direction of a linear relationship between two variables, was calculated to observe the strength of association between the millivolt reading and the temperature during calibration.

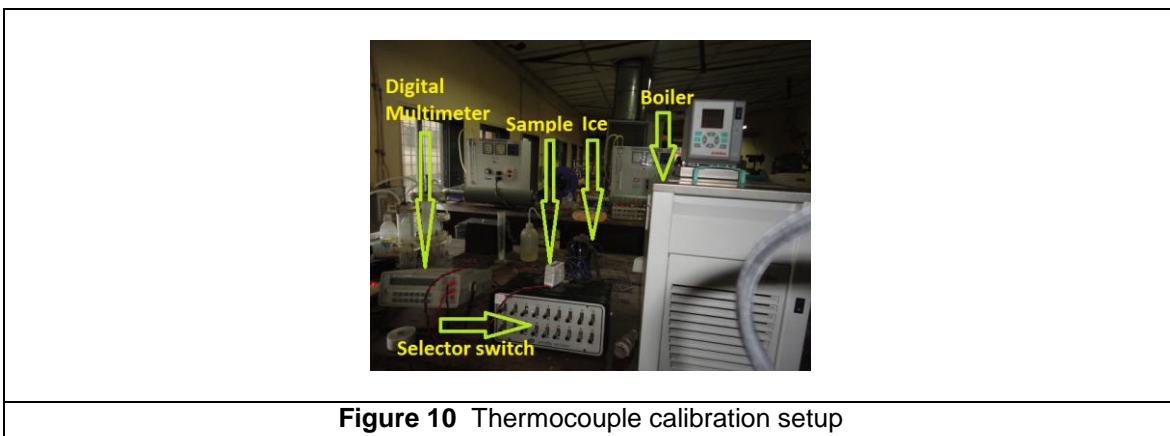
$$R = \frac{n(\sum T * V) - (\sum T) * (\sum V)}{\sqrt{n(\sum T^2) - (\sum T)^2} \sqrt{n(\sum V^2) - (\sum V)^2}}$$

Where

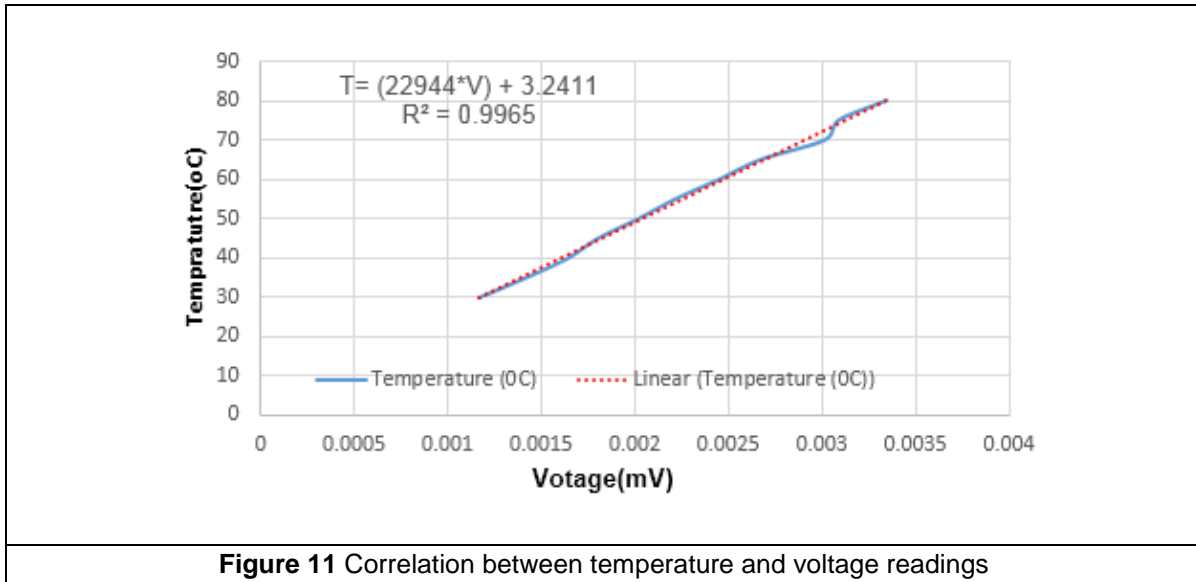
n is number of pairs of data

T is temperature in °C

V is voltage in mV



The thermocouple voltage at various known temperatures was measured. This will develop a correlation between thermocouple voltage and thermocouple temperature. This correlation is represented by the graph in figure 11. As it can be seen from the graph that the variation in temperature corresponds to the variation in voltage reading.



The end result of regression analysis predicts the value of an output variable (temperature) based upon the values of input variables (mV reading). So based on the result of the regression which is 99.6% the total variation in temperature can be explained by the linear relationship between mV readings and temperature readings. It can be clearly observed from the graph in figure 13 that the regression line passes almost exactly through every point on the scatter plot. So it can be concluded that this can be able to explain all the variations.

Table 3 shows the final result of correlation coefficient which is 0.998232 and this value indicates a strong positive linear relationship via a firm linear rule.

Table 3 Correlation coefficient of the curve fit

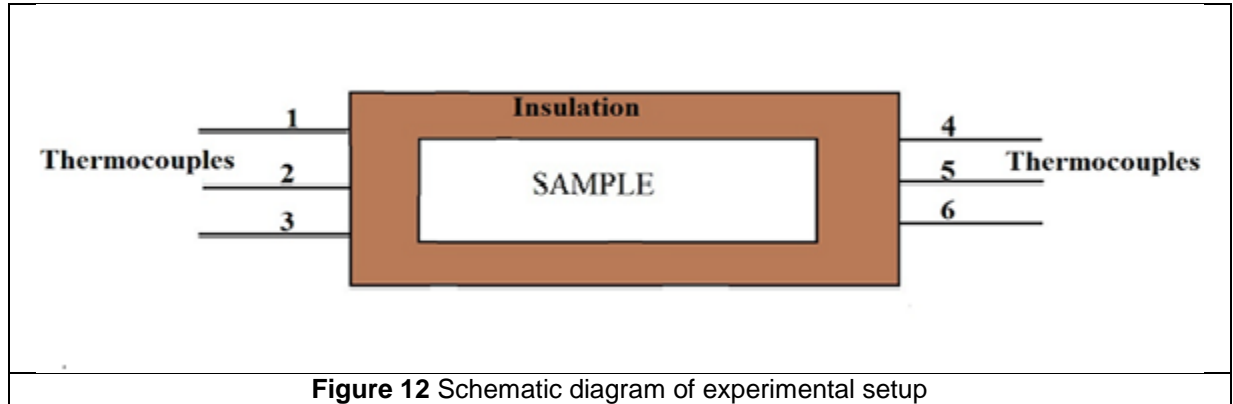
	Voltage (mV)	Temperature(°C)
Voltage (mV)	1	
Temperature(°C)	0.998232	1

4.2 Heat Conduction Test

Aluminum alloy 4043 which has 5% Si is used in this deposition. This alloy is used to weld many similar and dissimilar cast and wrought Al parts. It is extensively used with the GTAW and GMAW processes with Argon as shielding gas. The original thermal conductivity of the welding wire is $163 \text{ Wm}^{-1} \text{ K}^{-1}$.

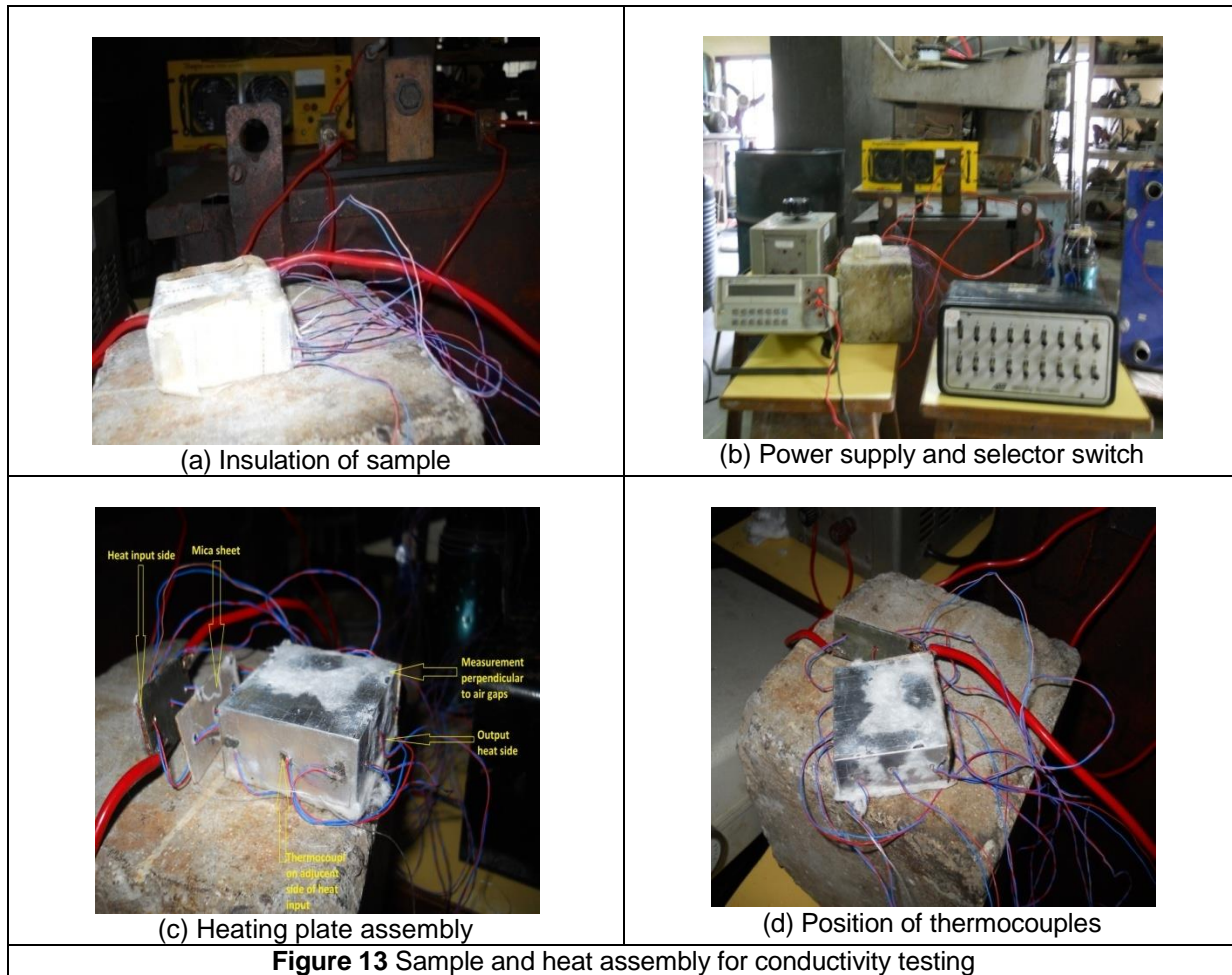
Six thermocouples are used to record the temperature difference on the heat input and output side of opposite faces of the sample as shown in figure 12. Three small holes, for three thermocouples on each side, with 3mm depth are drilled into four sides of the sample. The three

fixed thermocouples T_1 , T_2 and T_3 are positioned along the heater section with a gap of 16mm in between them. The other thermocouples T_4 , T_5 and T_6 are attached to the output side at similar intervals. The thermocouples on the input and output sides were connected to the selector switch for sequential selection and recording of the voltage readings.

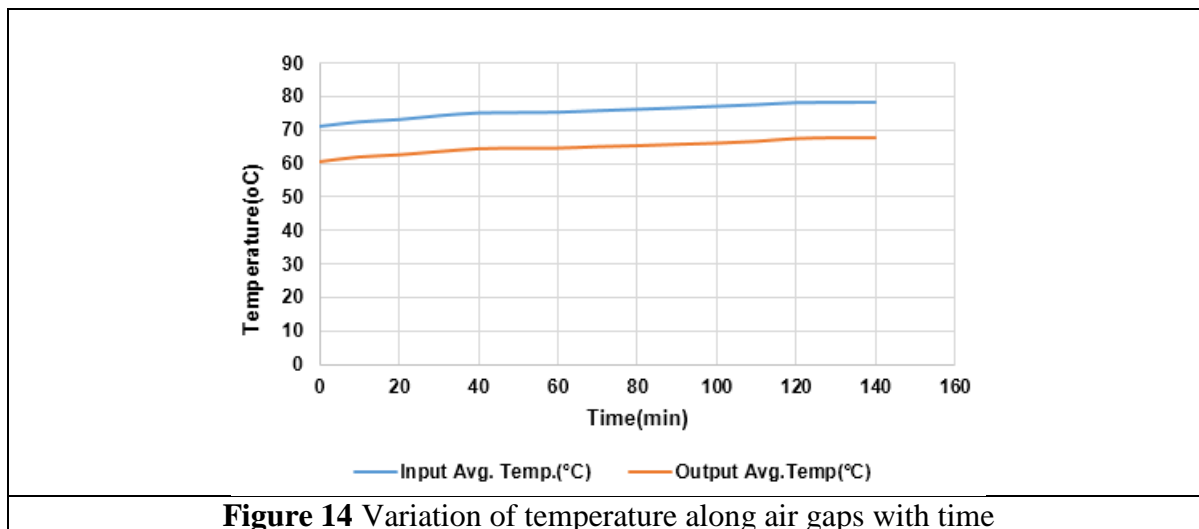


The apparatus consist of heating elements fitted on one side of the sample whose thermal conductivity has to be measured. The heater plate assembly is made up of mica sheets on which the Nichrome sheet is sandwiched in between upper and lower mica sheets for stabilizing and avoiding damage of the thermocouples. The sample was insulated on all of its faces for preventing the heat loss to the environment. When power is supplied to the heater, heat transfer will take place from the heat input side to the output side. The temperature of the sample is measured at the six positions by using a K type thermocouples and digital voltmeter. The power supply is adjusted to desired quantity by means of electronic controlled circuit by adjusting the voltage and current so as to provide the required watts of input to the heater plate. Electric power input can be measured by using digital voltmeter and ammeter multiplier [12]. The steady state temperature was ensured by the change in the voltage reading for each thermocouple which is fitted at the surface of the specimen. Steady state is reached when these voltmeter readings stop changing with time.

The rectangular sample was surrounded by a glass wool with a very high insulating capability as shown in figure 13(a). A glass tape was used to tightly hold the sample with the heating assembly and the insulating material. Temperature differences are measured by the calibrated thermocouples which are attached at the heat input and output sides of the specimen.



Variation of input and output temperature along air gaps with respect to time is shown in figure 14, it shows that almost constant temperature difference maintained between heat input and output side.



Variation of input and output temperature across air gaps with respect to time is shown in figure 15, it shows that almost constant temperature difference maintained between heat input and output side.

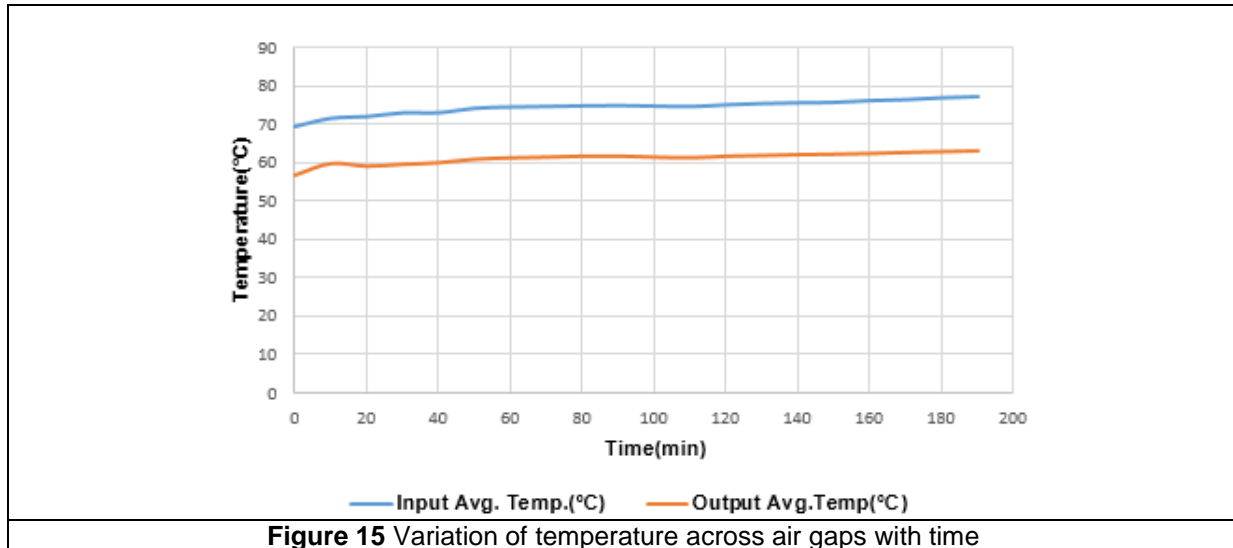


Figure 15 Variation of temperature across air gaps with time

As explained in the previous sections the main objective of this experiment is to prove the capability of *HLM* in producing directionally conductive material and to measure the directional conductivity of the sample in two different directions. It was assumed that the small variation in the air gap width due to spattering of molten metal to adjacent weld beads is negligible. For the measurement of thermal conductivity (*K*) one dimensional heat flow through the rectangular specimen was considered. Fourier’s law of heat conduction was considered throughout the heat conduction test.

4.2.2 Experimental Results

The experimental results for the DHC specimen showed anisotropic heat conduction measured through the opposite sides. A heat input of 30.4 watt was provided from one side of the specimen and the temperature difference across the specimen was measured. The input and output measured temperatures were averaged after steady state condition was reached. The variation of average temperature with time along and across air gaps shows a similar trend. Variation of temperature along and across air gaps with time is shown in figure 16. It shows output average temperature along air gap is more than that of temperature across air gap, which implies thermal conductivity across gap is less than that of across air gap.

Where:

$Q =$ heat transfer rate = $V.I = 30.4$ Watt,

$A =$ Area normal to heat transfer, m^2

$T_h =$ temperature of hot plate i.e. $(T_1 + T_2 + T_3) / 3$ in $^{\circ}C$

$T_c =$ temperature of cold plate i.e. $(T_4 + T_5 + T_6) / 3$ in $^{\circ}C$

$L =$ thickness of specimen along heat flow in m

To check the uni-directional heat flow, the temperature was measured on the adjacent side of the heat input side and a negligible heat flow was observed.

The measured value of thermal conductivity was $0.1398 \text{ Wm}^{-1} \text{ }^{\circ}\text{C}^{-1}$, which is negligible when

compared to heat flow on the heat input side. The variation of temperature along adjacent side of heat input is shown in figure 17, it shows there is negligible temperature difference between heat input and adjacent side.

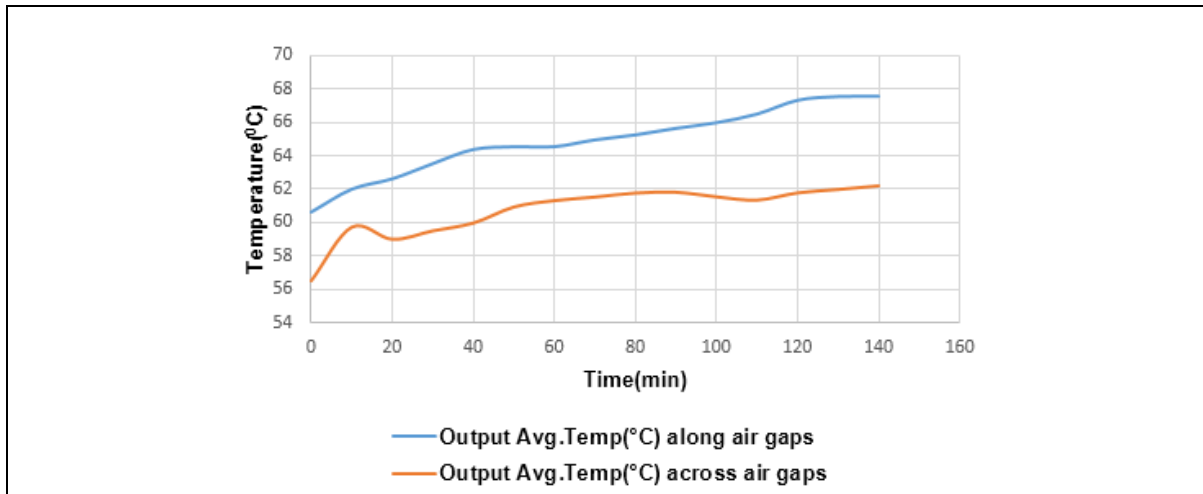


Figure 16 Variation of temperature along and across air gaps with time

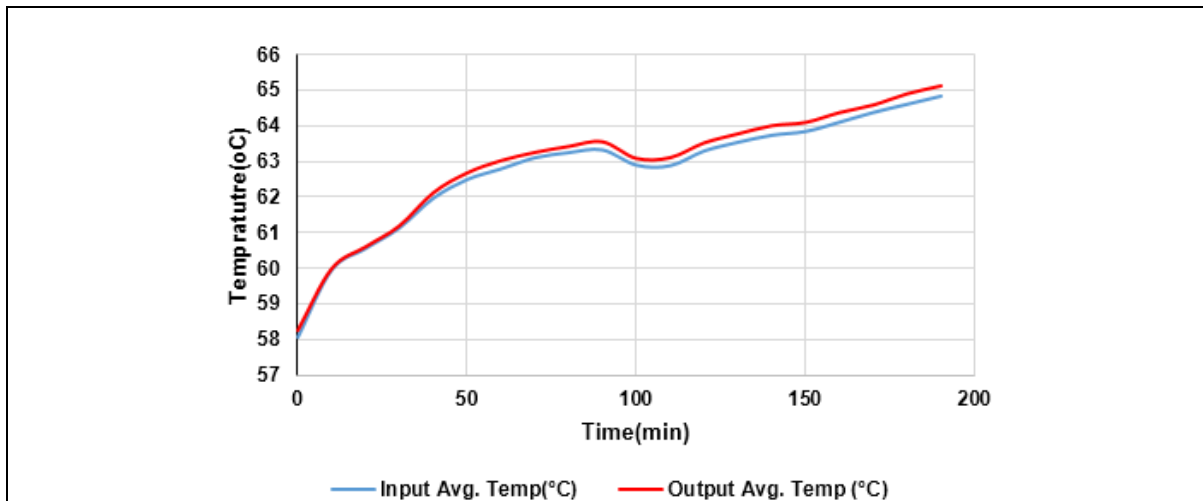


Figure 17 Variation of temperature along adjacent side of heat input

5. Conclusion

Unlike other heat sink, which radiates from all surfaces and in all directions, the new object developed through *HLM* radiate elaborately in one direction. The Al-Si alloy transfer heat away from the source along the welding direction but only minimally in a direction transverse to the welding direction. The object has demonstrated heat transfer of 130 W/m-k measured parallel to air gaps and 100 W/m-k perpendicular to air gaps. In general, the value of heat conductivity parallel and perpendicular to air gaps on the specimen was showed anisotropic thermal conductivity. The thermal conductivity was decreased by 37% in direction perpendicular to the air gaps and 20% in direction parallel to the air gaps.

References

1. Cengel, Y. A. (2003) "Heat transfer: a practical approach", 2nd edition, McGraw Hill, New York.
2. Lefrane, G., Degisher, H.P., Sommer, K.H., Mitic G. (1999), "Al-SiC improves reliability of IGBT power modules", *Proceedings of ICCM conference-2012*, Paris, Paper ID 1335.
3. Simancik, F. (2003) "Factors influencing the development of advanced metallic material in advanced metallic materials", proceedings of the international conference, Smolenice, 5-7 November, 2003. Bratislava.
4. Amiri, H., Mansouri, S.H., Safavinejad, A. (2010), "Combined conductive and radiative heat transfer in an anisotropic scattering participating medium with irregular geometries", *International Journal of Thermal Sciences*, Volume 49, Issue 3, pp. 492–503.
5. Gillet, J., Djafari-Rouhani, B., Pennec, Y. (2009), "Directional Thermal Conductivity of a Thin Si Suspended Membrane with Stretched Ge Quantum Dots", *EDA Publishing/THERMINIC 2009*, ISBN: 978-2-35500-010-2
6. Saban, D., Cloud, A., Guedes-Pinto, P., (2009), "Highly Conductive Insulation for Large, High-Speed Machines", Presented at the *Coil Winding / Insulation & Electrical Manufacturing Exhibition*, May 5-7, 2009, Messe Berlin, Germany.
7. Iyengar, M. (2007), "Design for Manufacturability of Forced Convection Air Cooled Fully Ducted Heat Sinks", available at <http://www.electronics-cooling.com/2007/08/design-for-manufacturability-of-forced-convection-air-cooled-fully-ducted-heat-sinks/> (accessed 3 November 2013).
8. Darfler, S., Valley, C., (1996), "High Thermal Conductivity of Non-Metallic Honeycomb", United States Patent, Patent Number: 5498462, Date of Patent: Mar 12 1996.
9. Korab, J., Stefanik, P., Kavecky, S., Sebo, P., Korb, G. (2002), "Thermal Conductivity of Unidirectional Copper Matrix Carbon Fiber Composites" *Journal of Composites*, Part A 33, pp.577-581.
10. Vos, D. L. (1999), "Thermally Conductive Vibration Isolators", United States Patent, Patent Number: 6002588, Date of Patent: Dec 19 1999.
11. Katsui, T. (2010), "Heat sinks and information processor using heat sinks", United States Patent no-7828045B2 ,Date of Patent: Nov 9,2010
12. Hamada, Y., Otsu, W., Fukai, J., Morozumi Y., Miyatake, O. (2005) "Anisotropic heat transfer in composites based on high-thermal conductive carbon fibres", *3rd International Symposium on Advanced Energy Conversion Systems and Related Technologies, Journal of Energy*, Volume 30, Issues 2–4, February–March 2005, pp 221–233.
13. Goldstein, R.J., Ibele, W.E., Patankar, S.V., Simon, T. W. (2006) "Heat transfer—A review of 2003 literature", *International Journal of Heat and Mass Transfer*, Volume 49, Issues 3–4, pp 451–534.
14. American Society for Testing and Materials, "Manual on the use of thermocouples in temperature measurement." *ASTM Committee E20 on Temperature Measurement*, 1993 ASTM International.
15. Suryakumar, S., Karunakaran, K.P., Bernard, A., Chandrasekhar, U., Raghavender, N. Sharma, D. (2011), "Weld bead modelling and process optimization in Hybrid Layered Manufacturing", *Journal of Computer- Aided Design* ,vol. 43,pp. 331-344.